High Affinity "Click" RGD Peptidomimetics as Radiolabeled Probes for Imaging $\alpha_v\beta_3$ Integrin[a]

Monica Piras,*[a] Andrea Testa, [a] Ian N. Fleming, [a] Sergio Dall'Angelo, [a] Alexandra Andriu, [a] Sergio Menta,[b] Mattia Mori,[c] Gavin D. Brown,[d] Duncan Forster,[d] Kaye J. Williams,[e] and Matteo Zanda*[a,f]

[a]	Dr. Monica Piras, Dr. Andrea Testa, Dr. Ian N. Fleming, Dr. Sergio Dall'Angelo, Alexandra Andriu and Prof. Dr. Matteo Zanda Institute of Medical Sciences and Kosterlitz Centre for Therapeutics School of Medicine, Medical Sciences and Nutrition University of Aberdeen, Foresterhill, Aberdeen, AB25 2ZD (Scotland, UK)
[b]	Dr. Sergio Menta* Dipartimento di Chimica e Tecnologie del Farmaco "Sapienza" Università di Roma, P.le A. Moro 5, 00185 Rome, Italy * Current affiliation: IRBM Science Park SpA, Via Pontina km 30,600 00071 Pomezia (RM), Italy
[c]	Dr. Mattia Mori Center for Life Nano Science@Sapienza Istituto Italiano di Tecnologia Viale Regina Elena 291, 00161 Roma (RM), Italy
[d]	Dr. Gavin D. Brown and Dr. Duncan Forster Manchester Cancer Research Centre and Wolfson Molecular Imaging Centre, The University of Manchester Palatine Road, Manchester, M20 3JJ (UK)
[e]	Prof. Dr. Kaye J. Williams CRUK-EPSRC Cancer Imaging Centre in Cambridge and Manchester, Manchester Cancer Research Centre Division of Pharmacy and Optometry The University of Manchester Oxford Road, Manchester, M13 9PT (UK)
[f]	Prof. Dr. Matteo Zanda C.N.R. – I.C.R.M., via Mancinelli 7, 20131 Milan (Italy)

Abstract: Non-peptidic RGD-mimic ligands were designed and synthesized by click chemistry between an arginine-azide mimic and an aspartic acid-alkyne mimic. Some of these molecules combine excellent *in vitro* properties (high $\alpha_v\beta_3$ affinity, selectivity, drug-like logD, high metabolic stability) with a variety of radiolabeling options (e.g. tritium and [18F]fluorine, plus compatibility with radio-iodination), not requiring the use of chelators or prosthetic groups. The binding mode of the resulting triazole RGD-mimics to $\alpha_v\beta_3$ or $\alpha_{IIb}\beta_3$ receptors was investigated by molecular modeling simulations. Compound **12** was successfully radiofluorinated and used for *in vivo* PET/CT studies in U87-tumour models, which showed only modest tumour uptake and retention, owing to rapid excretion. These results demonstrate that the novel click-RGD mimics are excellent radiolabeled probes for *in vitro* and cell-based studies on $\alpha_v\beta_3$ integrin, whereas further optimization of their pharmaco-kinetic and dynamic profile would be necessary for a successful use in *in vivo* imaging.

Introduction

Integrin $\alpha_v\beta_3$ is a heterodimeric transmembrane protein that belongs to the integrin superfamily receptors.[1,2] This integrin subtype attracted considerable attention because it plays a key role in tumour angiogenesis, growth and metastasis, and in the last two decades it has become an established target for tumour treatment and diagnosis.[3,4] Integrin $\alpha_v\beta_3$ is a receptor for multiple components of the extracellular matrix, including vitronectin, fibrinogen and fibronectin, that expose the Arg-Gly-Asp (RGD) tripeptide sequence.[5] The ligand-receptor recognition process is mainly regulated by the aspartic acid carboxylic group and the arginine guanidine group, both forming ionic interactions with a charged region of the protein.[6] These two moieties need to be separated by a 12–14 Å distance to allow the correct fitting into the $\alpha_v\beta_3$ binding pocket.[7] Although a number of high affinity RGD peptides have been described and some of them advanced to clinical trials,[8] RGD peptide mimics may offer significant advantages such as having better drug-like properties and allowing more flexibility in the exploration of optimized structure-activity-relationships with the receptor.[9] Structural modifications made on the linear pharmacophore consist of variation of the flanking amino acids and introduction of structural constraints, which were achieved by cyclization or by insertion of a rigid moiety (e.g. phenyl, isoxazole, 1,2,3-triazole rings and hydrazide bonds) in the flexible peptide sequence.[9–13] In fact, the reduction of conformational freedom towards a correct bioactive orientation favorably affects both activity and selectivity. From several studies focusing on the development of non-peptide RGD mimics, L-2,3-diaminopropanoic acid emerged as an optimal replacement of aspartic acid. Likewise, the substitution of the Arg guanidine function with less basic moieties

---

[a] Supporting information for this article is given via a link at the end of the document.

(2-aminoimidazoles, 2-aminopyridines) has been proposed.[10,11] To improve the pharmacological features of RGD peptides, a number of RGD peptidomimetics have been developed as therapeutic agents.[14] However, relatively few studies have investigated the use of these molecules as radiotracers.[15–20] Kessler and co-workers assessed the potential of non-peptidic RGD mimics as PET imaging agents by equipping the integrin antagonists with a bifunctional chelator (NODAGA) and labeling with ^{68}Ga^{3+}.[21] More recently, the direct radioiodination of non-peptide integrin ligands has been reported and the resulting tracers assessed as SPECT imaging agents.[22] In this study we designed small-molecule RGD-mimics that combine excellent biological properties (high affinity, selectivity, suitable logP value) with a variety of radiolabeling options not requiring the use of chelators or prosthetic groups. To this end, a small library of RGD peptidomimetics was synthesized and biologically screened to identify the chemical modifications that confer the highest $\alpha_v\beta_3$ affinity and selectivity against integrin $\alpha_{IIb}\beta_3$, which mediates platelet aggregation. The main features of these novel RGD mimics are: (a) α-N-(arylsulfonyl)-L-2,3-diaminopropanoic acid and 2-amino-3-methyl pyridine as Asp and Arg substituent, respectively; (b) a distance of about 13 Å between the acidic and basic groups in the predicted binding conformation; (c) a triazole ring as Gly mimetic, which confers favorable conformational restrictions to the linear scaffold and provides a versatile labeling site for the incorporation of tritium[23] and iodine[24] radioisotopes; (d) an electron-poor aromatic ring activated for ^{18}F-labeling via nucleophilic aromatic substitution[25] on the Asp-mimic portion (Figure 1). Notably, molecular modelling studies suggest that this fluorine atom may significantly contribute to the affinity and selectivity of these ligands through an attractive electrostatic interaction with the Tyr178 hydroxyl group of the α_v subunit.
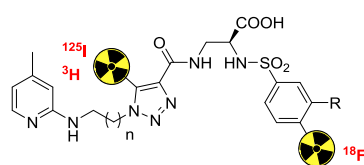

Figure 1. Structural scheme of triazole based RGD mimics with the triazole ring as labeling site for tritium or iodine radioisotopes and phenyl ring as labeling site for ^{18}F.

Results and Discussion

Design and Synthesis. The copper-(I)-catalyzed 1,2,3-triazole cycloaddition allowed a convenient assembly of all the target compounds via "click chemistry" (Scheme 1). Two regioisomers (**1** and **2**) were initially prepared by swapping the orientation of the triazole ring (Figure 2). The higher affinity ligand **1** was then selected for the optimization of the biological properties and the design of labeled derivatives **12** and **15**.
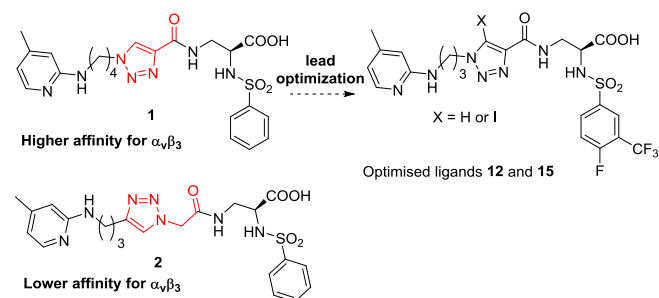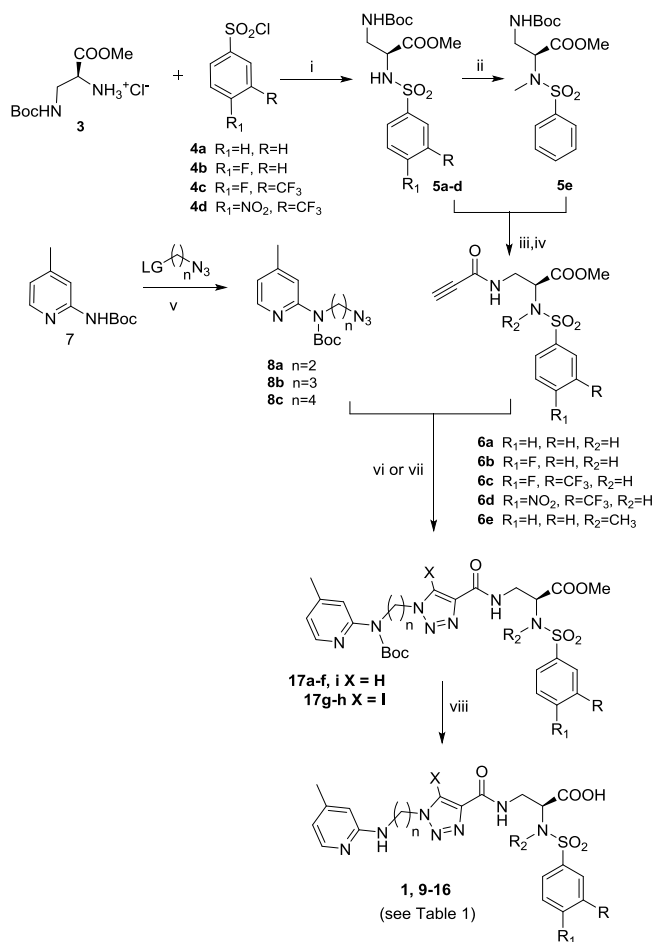

Figure 2. Triazole based RGD mimic regioisomers **1** and **2** and evolution of 1 into the optimized $\alpha_v\beta_3$ ligands **12** and **15**.

The synthesis of compound **1** and its analogues **9–16** (substituents shown in Table 1) is outlined in Scheme 1. The synthesis of the alkyne building blocks started from commercially available (S)-methyl-2-amino-3-($tert$-butoxycarbonylamino)propanoate hydrochloride (**3**) that was reacted with arylsulfonyl chlorides **4a–d** to give sulfonamides **5a–d**. N-methylation of the sulfonamide function of **5a** afforded the intermediate **5e**. After acidic removal of the N-Boc protecting group from **5a–e**, an amide-forming coupling was performed with propiolic acid, leading to the desired alkyne intermediates **6a–e**. The click partners **8a–c** were synthesized by alkylation of N-Boc protected 2-amino-3-methylpyridine **7**. Coupling of alkynes **6a–e** with azides **8a–c** via CuAAC reaction afforded 1,2,3-triazole intermediates **17a–f** and **17i**. The iodinated 5-iodo-1,2,3-triazole analogues **17g–h** were prepared by coupling alkynes **6a** and **6c** with the corresponding "click partners" **8c** and **8b** - respectively - in the presence of CuI, N-iodosuccinimide (NIS) and trimethylamine. Treatment of the methyl ester and N-Boc protected intermediates (**17a–i**) with LiOH followed by TFA afforded the desired products **1** and **9–16** (for structural details see Table 1).

Scheme 1. Synthesis of compound **1** and its analogues (**9–16**). LG = Leaving Group. *Reagents and conditions*: (i) TEA, DCM, 12h, 0°C to room temp (78–99%); (ii) K_2CO_3, TEBA, MeI, CH_3CN, 2h, room temp (85%); (iii) TFA/DCM 1:2, 2h; (iv) EEDQ, propiolic acid, DCM, 1h (50–90%); (v) NaH, K_2CO_3, DMF, 1.5 h (90–95%); (vi) $CuSO_4$ (2%), Na ascorbate (10%), *t*BuOH/H_2O 2:1, 12h (60–98%) ; (vii) NIS, CuI, TEA, CH_3CN, 2h (45–47%) (viii) LiOH, H_2O/THF 1:2, 20 min then TFA/DCM 1:1, 2h (quantitative yields).

The regioisomer **2** was prepared by swapping the functionalization of the "click partners" relative to **1**, namely incorporating the azide moiety on the Asp-mimic fragment **18** and the alkyne counterpart on the Arg-like side chain (**19**). Alkyne **19** was prepared from **7** as already described.[23] The synthesis of the azide fragment **18** was accomplished by coupling of azidoacetic acid with the amine **20**, that was prepared according to the literature.[26] "Click"-cycloaddition of the azide **18** with the alkyne **19** gave the 1,2,3-triazole **21**. Treatment of **21** with TFA afforded the desired deprotected regioisomer **2** (Scheme 2).
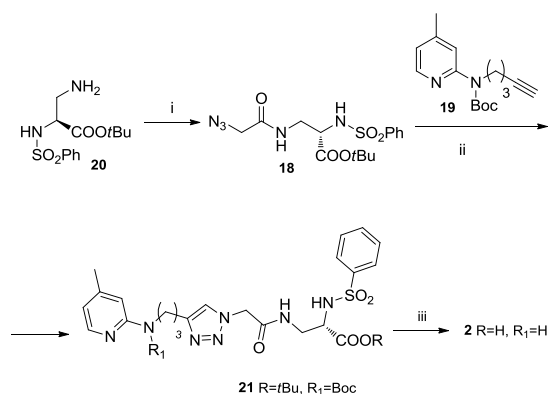
Table 1. IC$_{50}$ values of triazole-based RGD peptidomimetics and *c*(RGDfK) pentapeptide concerning the inhibition of *c*[RGDfK(Biotin-PEG-PEG)] peptide and biotinylated fibrinogen binding to the isolated α$_v$β$_3$ and α$_{IIb}$β receptors, respectively.

entry	comp	structure	IC$_{50}$[a] α$_v$β$_3$ (nM)	IC$_{50}$[a] α$_{IIb}$β$_3$ (nM)	SI[c]
1	**10**		900 ± 8	6090 ± 135	6.8
2	**9**		57 ± 1	670 ± 1	12
3	**1**		110 ± 56	500 ± 3	4.5
4	**11**		81 ± 51	1845 ± 63	23
5	**12**		25 ± 3	11690 ± 2840	467
6	**13**		10 ± 3	24400 ± 450	2444
7	**14**		110 ± 34	2450 ± 1390	22
8	**15**		10 ± 1	6670 ± 21	667
9	**16**		3600 ± 18	-	-
10	**2**		640 ± 12	-	-
11	***c*[RGDfK]**		138 ± 51	20250 ± 4630	146

[a] IC$_{50}$ values were calculated as the concentration of ligand required for 50% inhibition as estimated by GraphPad Prism software. Each data point is the average from multiple independent experiments, performed in triplicate. [b] Selectivity Index (SI) = IC$_{50}$ α$_{IIb}$β$_3$/ IC$_{50}$ α$_v$β$_3$.

Scheme 2. Synthesis of **2**. Reagents and conditions: (i) azidoacetic acid, DCC, DCM, 12 h (99%); (ii) CuSO$_4$ (2%), Na ascorbate (10%), *t*BuOH/H$_2$O 2:1, 12 h (90%); (iii) TFA/DCM 1:1, 3 h (quantitative yield).

To investigate the possibility of radio-iodinating these RGD-mimics, preliminary studies were performed using cold non-radioactive conditions, applying a synthetic procedure reported by Årstad *et al* for the synthesis of imaging agents containing a 5-[^{125}I]Iodo-1,2,3-triazole group.[24] The click reaction between alkyne **6a** and azide **8c** was performed in the presence of a stoichiometric amount of CuCl$_2$, TEA (1.5 equiv) and NaI (1 equiv). The reaction was monitored *via* LC-MS (Fig. S1 top panel, Supporting Information) showing the non-iodinated triazole analogue **17a** (R, R^1, R^2, X = H, n=4) as the major by-product. In order to optimize the labeling conditions, chloramine-T (1 equiv) was employed as an oxidizing agent and tetrakis(acetonitrile)copper(I) hexafluorophosphate ([Cu(CH$_3$CN)$_4$]PF$_6$) (1 equiv) as a source of copper(I). Under these conditions the iodinated compound **17g** (R, R^1, R^2 = H, X = I, n=4) was detected as the major peak in the HPLC chromatogram (see Fig. S1 bottom panel, Supporting Information) with no observed **17a** formation.

Receptor binding assays. The design of triazole containing RGD-mimics afforded a set of 10 molecules that were submitted to competition binding assays to determine their binding affinity toward integrin α$_v$β$_3$[27] and selectivity over the closely related integrin α$_{IIb}$β$_3$. Results are reported in IC$_{50}$ values (Table 1). Cyclic *c*[RGDfK] was included in the tests as positive control in order to compare the new RGD mimics with a well-established rigid ligand. These tests showed that ligand length (n) has a significant impact on α$_v$β$_3$ affinity (entries 1–3), and a propyl chain (n = 3, entry 2) was found to provide the optimal distance between the Asp- and Arg-mimetic fragments to allow a correct fitting of the ligand into the binding pocket. Interestingly, the activity on α$_v$β$_3$ and the selectivity against α$_{IIb}$β$_3$ seem to be strongly dependent on the substitution of the phenyl ring with fluorine and EWGs such as nitro (NO$_2$) and trifluoromethyl (CF$_3$) moieties (entries 4–6). An increased affinity (2 to 4-fold) and a remarkable improvement in selectivity (up to 36-fold) were, in fact, observed in this series of derivatives (compare entry 2 with 4–6**)**.

The IC$_{50}$ values of iodinated peptidomimetics **14** and **15** compared with their non-iodinated analogues **1** and **12** revealed that incorporation of iodine on the triazole ring did not affect affinity and selectivity (entries 3 *vs* 7 and 5 *vs* 8). Conversely, the *N*-methyl sulfonamide derivative **16** showed a considerable drop in affinity (entry 9), confirming the crucial role that the free sulfonamide function -NHSO$_2$- plays in ligand-receptor interactions. Comparison of the IC$_{50}$ values of non-peptide ligands **12**, **13** and **15** with that of *c*(RGDfK)

reference peptide (entry 11) indicates a considerable increase of binding affinity for $\alpha_v\beta_3$ in this series of analogues (to almost 14-fold) as well as an enhanced selectivity over $\alpha_{IIb}\beta_3$.

Molecular Modelling. To provide structural support to biological activity data shown in Table 1, the binding mode of triazole RGD-mimics to $\alpha_v\beta_3$ or $\alpha_{IIb}\beta_3$ receptors was investigated by molecular modeling simulations. Entries 1–10 were docked towards the crystallographic structure of each receptor,[6,28] and lowest energy poses were further relaxed by extensive energy minimization.

Ligand theoretical affinity was computed by the MM-GBSA[29,30] and XSCORE[31] methods providing a very good correlation with experimental inhibitory activity data ($R^2 = 0.896$ and $R^2 = 0.662$, respectively (see also Supporting Information). Notably, the predicted binding mode of RGD-mimics is highly comparable with that of the crystallographic RGD ligand,[6] since they establish canonical interactions with the $\alpha_v\beta_3$ receptor as observed for well-known inhibitors. However, molecular docking suggested that triazole RGD-mimics **11**, **12**, **13** and **15** bearing a *nitro* group or fluorine atoms substituted at the phenyl ring are able to form an additional H-bond interaction with the side chain of Tyr178 (α_v subunit) (Figure 3). This interaction has never been exploited before for improving the affinity of integrin inhibitors and, in agreement with biological activity data of Table 1 and theoretical binding affinity (see Supporting Information), it may be responsible for the higher inhibitory potency against the $\alpha_v\beta_3$ receptor displayed by these molecules. Most notably, Try178 is missing on the $\alpha_{IIb}\beta_3$ receptor, where it is replaced by Phe160 that is however unable to establish H-bond interactions with these RGD-mimics, thus providing a structural explanation to the high selectivity for $\alpha_v\beta_3$ observed for **11**, **12**, **13** and **15**.

Iodine substitution is another unique feature of these triazole RGD-mimics, which was found to increase the binding affinity of **15** by experimental and molecular modelling studies (compare entry 5 with 8). Indeed, the iodine atom in **15**, the most potent RGD-mimic of this series, is able to establish hydrophobic interactions with Tyr178 and Trp179 (α_v) and Ala218 (β_3 subunit). In contrast, iodine substitution in RGD-mimic **14**, which bears a four-carbon linker, did not provide affinity gain, as the iodine is exposed to the solvent due to steric restrictions imposed by the length of the linker (compare entry 3 with 7, see also Supporting Information).

The sulfonamide group of all molecules but **16** contacts the backbone of Asn215 and the side chain of Arg214 of the β_3 subunit by H-bonds, thus providing a rational explanation for the loss of inhibitory activity observed upon methylation of the sulfonamide NH function (compare entry 2 with 9).

For additional details on binding modes and theoretical affinities see the Supporting Information.
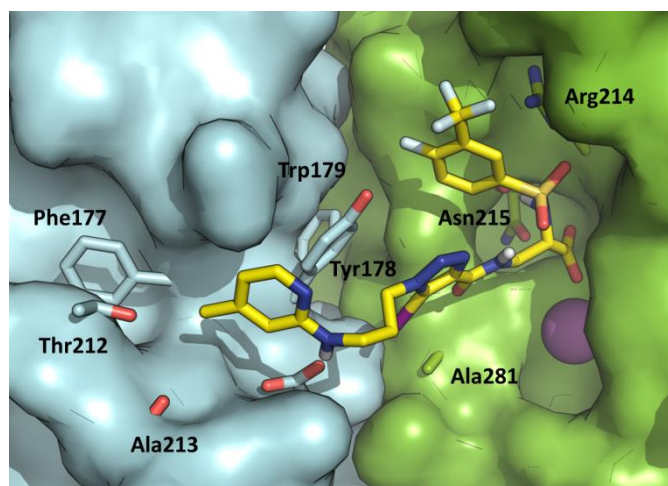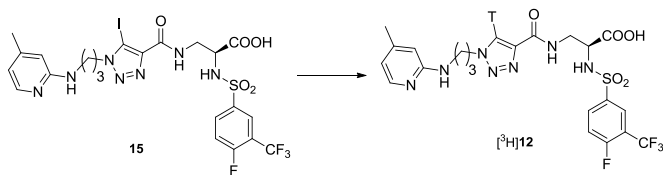

Figure 3. Predicted binding mode of RGD-mimic **15** (yellow sticks) on the crystallographic structure of $\alpha_v\beta_3$ receptor (PDB: 1L5G). α_v and β_3 subunits are colored cyan and green, respectively. Residues contacted by RGD-mimics are shown as sticks and labeled. The divalent cation in the MIDAS region is shown as a violet sphere.

Labeling. Based on the affinity data discussed above, compounds **12** and **15**, which are fluorinated and iodinated versions of the initial lead **1**, represent potential radiotracers for PET and SPECT imaging. Furthermore, tritiated versions could be useful tools for *in vitro* studies. We therefore investigated the synthesis of **12** and **15** in different radiolabeled forms (tritiation and radiofluorination).

Tritiation. Compound **12** was successfully labeled with tritium (Scheme 4). To the best of our knowledge this is the first example of ^{3}H-labeled non peptidic molecule able to bind integrin $\alpha_v\beta_3$, therefore [^{3}H]**12** may represent a very useful tool for *in vitro* or *ex-vivo* studies on angiogenesis. The palladium-mediated dehalogenation was accomplished on the 5-iodotriazole **15** employing tritium gas in a tritium handling manifold in the presence of Pd/C and TEA (excess) in ethanol. Complete conversion of the iodinated starting material was obtained after 2.5 hours and the desired product was isolated by analytical HPLC with a radiochemical purity > 99% and a specific activity of 469 GBq/mmol.

Scheme 4. Synthesis of [³H]**12**. Reagents and conditions: Pd/C cat, TEA, ³H₂, EtOH, 2.5 h, room temp.

A logD (pH 7.4) = -0.55 was experimentally measured for [³H]**12** (see Supporting Information for details). The compound was evaluated in cells that are known to express no, moderate and very high levels of $\alpha_v\beta_3$ integrin.[32,33] The magnitude of [³H]**12** binding to each cell line was consistent with $\alpha_v\beta_3$ expression levels (Figure 4A). Non-radiolabeled *c*(RGDfK) (10µM) was included to competitively block specific binding to $\alpha_v\beta_3$. This decreased [³H]**12** binding to PC3 and U87MG cells by approximately 60%, but had no effect in MCF7 cells (Figure 4B).
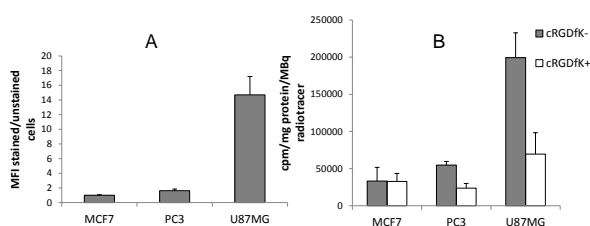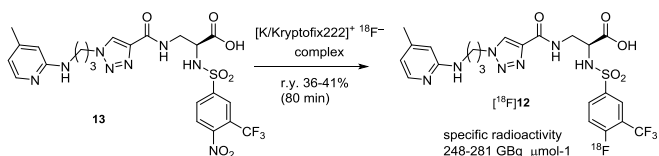

Figure 4. (A) Characterization of $\alpha_v\beta_3$ expression on MCF7, PC3 and U87MG cells. Results are expressed as Median Fluorescence Intensity (MFI) of stained/unstained cells. (B) Cells were incubated with [³H]**12** in the presence (+) or absence (-) of 10 µM *c*(RGDfK) peptide for 1h. [³H]**12** binding is expressed as counts per minutes (cpm), as a function of the radioactivity added/plate and normalized for protein content. Each data point is the average ± standard deviation of at least three independent data points. T-test: Binding in presence vs absence of *c*(RGDfK) peptide; MCF7 p>0.05; PC3 p<0.001, U87MG p<0.0001.

¹⁸F-radiolabeling. Radiolabeling of compound **12** with ¹⁸F-fluorine-was achieved *via* [¹⁸F]-fluoride nucleophilic substitution using the nitro derivative **13** as precursor (Scheme 5).

Scheme 5.

The radiosynthesis was performed as a one-pot, two-step method using the Tracerlab FX-FN platform (GE Healthcare). For the initial step, a [K/Kryptofix222]⁺ ¹⁸F⁻ complex was prepared and dried azeotropically under a stream of helium and vacuum at 110 °C.
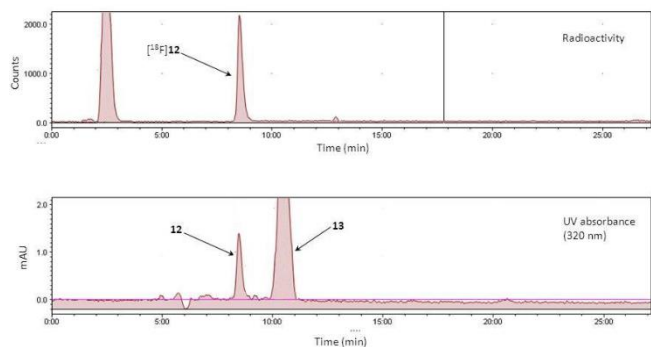

Figure 5. Radio-RP-HPLC analysis of [¹⁸F]**12** (above) and its UV profile (below).

Second, [18F]**12** was prepared by Kryptofix-mediated [18F]nucleophilic fluorination at the nitro position of **13**. Isolation of pure [18F]**12** was achieved by semi-preparative reverse phase HPLC (Fig. 5). The isolated product was then eluted through a C18 SEP-PAK to remove the HPLC eluent and formulated in a mixture of 0.9% saline/ethanol (92:8) for preclinical application. After radioactive decay, the cold [19F]**12** - which had formed in the radiofluorination concomitantly with [18F]**12** - was analyzed by proton-decoupled 19F-NMR (376 MHz) to verify the fluorination position (for a copy of the spectrum see Fig. S5, Supporting Information). A single peak at -110.1 ppm was observed, having the same chemical shift as the fluoro group of authentic **12**. The radiochemical yield (decay corrected) of [18F]**12** from nucleophilic [18F]fluoride was 36-41% giving 2.54-2.90 GBq (n = 8) of product at the end of the radiosynthesis (EOS). The radiochemical purity was ≥99%, and the specific radioactivity was 248-281 GBq μmol^{-1} (EOS). The total radiosynthesis time was approximately 80 min.

In vivo Imaging. Promising *in vitro* data and successful 18F-radiolabeling prompted pilot *in vivo* analyses. Four mice implanted with U87 tumour xenografts on the back were subjected to PET/CT imaging with [18F]**12**. Overall tumour retention of the tracer was low throughout the dynamic scan, whereas clearance was rapid, exhibiting both hepatobiliary and renal excretion. Uptake was initially high in the kidneys and liver but dropped off over the course of the 90 mins scan (Fig. 6). By 10 mins most of the injected dose could be found in the urinary bladder, where by 90 mins virtually all of the activity could be detected (Fig. 6 A). The low *in vivo* tumour uptake (0.9 ± 0.1%ID/g) and retention of [18F]**12** appears to be partly due to low bioavailability resulting in rapid excretion. The rapidity of this process and lack of kidney retention suggest that the molecule is excreted unchanged without any prior metabolism. This hypothesis is supported by human and rat liver microsomal (HLM / RLM) stability tests performed on **12**, whose half-life upon incubation with HLM and RLM at 37 °C in the presence of the co-factor NADPH was very high, namely 770 and 470 min, respectively, as detected by LC-MS/MS analysis. In comparison, in similar U87-MG mouse xenograft models [18F]fluciclatide was reported to have a tumour-retention comprised between 1.28 ± 0.34 %ID/g and 1.88 ± 0.73 %ID/g (13 days later) 90 mins after injection.[34]

Autoradiography. Sections of the U87-cells-derived tumors were mounted on slides and – after standard preparations - treated either directly with [18F]**12** or [18F]**12** incubation combined with cold **12** for determining the presence of non-specific binding. After overnight exposure to [18F]**12** the sections treated with [18F]**12** alone showed greater overall binding than the sections treated with an excess of cold **12** as well (Fig. 6B), indicating specific binding to $\alpha_v\beta_3$ integrin comparable to that observed in *in vitro* studies. Expression of integrin $\alpha_v\beta_3$ in the U87 tumour xenografts used was confirmed by immunohistochemical staining (see Fig. S3, Supporting Information).
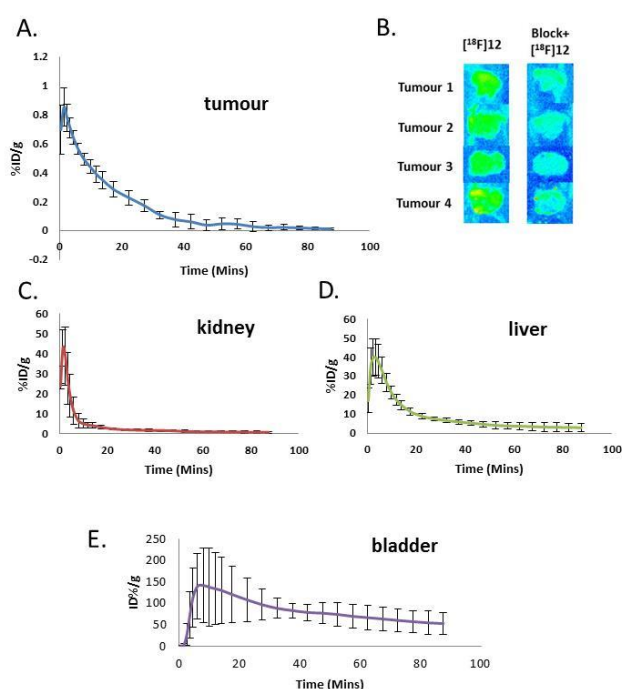

Figure 6. Time-activity curve of [18F]**12** tumour uptake in U87 xenograft tumors (A).. Pre-treatment of U87 tumour sections with cold **12** ("block") reduces [18F]**12** binding (B). C-E Time-activity curves of kidney, liver and bladder. Data in A, C -E are mean values obtained from 4 mice. Error bars indicate SD.

Conclusions

Novel small-molecule RGD mimics were designed and synthesized by click chemistry between an arginine-azide mimic and an aspartic acid-alkyne mimic. Some of these compounds displayed excellent *in vitro* properties (high $\alpha_v\beta_3$ affinity and selectivity, drug-like logD,

high HLM/RLM stability), are amenable to radiolabeling with iodine, or tritium, or [^{18}F]fluorine, and do not require the use of chelators or prosthetic groups. Molecular modeling simulations provided an insight into the binding mode of these compounds to $\alpha_v\beta_3$ or $\alpha_{IIb}\beta_3$ receptors. Compound **12** was successfully radiofluorinated and used for *in vivo* PET/CT studies in U87-tumour models, which showed only modest tumour uptake and retention, partly owing to rapid excretion through the kidneys into urine. The results above demonstrate that the novel click-RGD mimics are excellent radiolabeled probes for *in vitro* and cell-based studies on $\alpha_v\beta_3$ integrin, whereas further optimization of their pharmaco-kinetic and dynamic profile will be required for a successful use in *in vivo* imaging *via* SPECT or PET/CT.

Experimental Section

Materials and instrumentation

Chemicals were purchased from Sigma Aldrich and Bachem. NMR spectra were recorded using a Bruker Avance-400 spectrometer equipped with a 5 mm single-axis Z-gradient quattro nucleus probe, operating at 376 MHz for ^{19}F NMR. The spectrometer was operated with TOPSPIN NMR software (Version 2.0). Chemical shifts (δ) are reported in parts per million (ppm), relative to trichloro-fluoro-methane (0.00 ppm).QMA SEP-PAK light cartridges and C$_{18}$ SEP-PAK plus cartridges were obtained from Waters (Milford, MA). No-carrier-added [^{18}F]fluoride was produced *via* the ^{18}O(p, n)^{18}F nuclear reaction by irradiation of a 95-97% [^{18}O]enriched water target with a 16.4 MeV proton beam on the GE PETtrace cyclotron at the Wolfson Molecular Imaging Centre, Manchester, UK. Automated synthesis of [^{18}F]12 was carried out using the Tracerlab FX-FN radiochemistry system. Purification of [^{18}F]12 by HPLC was carried out on the same system equipped with a preparative reverse phase C$_{18}$ column (Prodigy ODS-Prep, 10μm particle size; 250 x 10 mm i.d.; Phenomenex, UK). For the purpose of quality control, HPLC analysis was carried out on a Shimadzu prominence system operated using LabLogic software (Laura 3.0) and configured with a CBM-20A controller, LC-20AB solvent delivery system and SPD-20A absorbance detector. The system was equipped with a C$_{18}$ Prodigy ODS(3) column, 5 μm particle size, 250 x 4.6 mm. Radioactivity was monitored with a radio-HPLC Bioscan Flowcount B-FC 3100 detector.

Chemistry.

Synthesis of 17e. Alkyne **6c** (67.5 mg, 0.17 mmol, 1 equiv) and azide **8b** (50 mg, 0.17 mmol, 1 equiv) were suspended in a mixture of *t*BuOH/H$_2$O 2:1 (3 mL/mmol). CuSO$_4$ (2%) and sodium ascorbate (10%) were added and the mixture was stirred at room temperature for 12 h. The reaction mixture was diluted with water, extracted with ethyl acetate (30 mL) three times and washed with brine. The collected organic phases were dried over Na$_2$SO$_4$, filtered and the solvent removed under vacuum. The crude mixture was purified by preparative thin-layer chromatography (PLC) (silica gel, n-Hex/EtOAc 4:6 as eluent) affording 96.5 mg (83% yield) of a white solid: R_f = 0.5 (*n*-Hex/EtOAc 3:7); ^{1}H NMR (400 MHz, CDCl$_3$) δ 8.24 (s, 1H), 8.20 (d, *J* = 5.1 Hz, 1H), 8.12 – 7.89 (m, 3H), 7.43 (s, 1H), 7.20 (t, *J* = 9.2 Hz, 1H), 6.89 – 6.84 (m, 2H), 4.49 (t, *J* = 7.1 Hz, 2H), 4.34 – 4.26 (m, 1H), 3.99 (t, *J* = 6.7 Hz, 2H), 3.91 – 3.72 (m, 2H), 3.65 (s, 3H), 2.43 – 2.21 (m, 5H), 1.50 (s, 9H); ^{19}F NMR (376 MHz, CDCl$_3$) δ -61.74 (d, *J* = 12.5 Hz), -107.17 (q, *J* = 12.5 Hz); ^{13}C NMR (101 MHz, CDCl$_3$) δ 170.1, 161.7 (d, *J* = 262.3 Hz), 161.0, 154.2, 153.9, 148.5, 147.2, 142.1, 137.2 (d, *J* = 3.8 Hz), 133.3 (d, *J* = 9.8 Hz), 126.9, 126.2, 121.6 (q, *J* = 273.3 Hz), 121.1, 119.9, 118.9 (dd, *J* = 34.0, 13.5 Hz), 117.9 (d, *J* = 21.8 Hz), 81.6, 56.2, 52.9, 48.7, 43.9, 41.2, 29.3, 28.3, 21.1; MS (ESI, *m/z*): C$_{28}$H$_{34}$F$_4$N$_7$O$_7$S [M+H]$^+$ calc. 688.21 found 688.2. [α]$_D^{25}$ = **-3** (c = 0.7, CHCl$_3$).

Synthesis of 12. The methyl ester and *N*-Boc diprotected intermediate **17e** (91 mg, 0.13 mmol) was dissolved in THF (0.2 M) and a solution of LiOH 4 M in water (500 μL/mmol) was added. The reaction mixture was vigorously stirred at r.t. After cleavage of the methyl ester function (20 min) the THF was removed *in vacuo* and the reaction mixture was partitioned between DCM and HCl (1 M aq.). The organic layer was dried over Na$_2$SO$_4$ and concentrated under low pressure. The resulting colourless oil was dissolved in a solution of TFA/DCM 1:1 and stirred for 2 h at r.t. for removal of the Boc protecting group. The solution was concentrated bubbling nitrogen into the flask and then lyophilized. After lyophilisation the product appeared as a white solid (90 mg, quantitative yield, MW = **12** · 1 TFA = 573.5 + 114 = 687.5): ^{1}H NMR (400 MHz, CD$_3$OD) δ 8.37 (s, 1H), 8.16 – 8.12 (m, 2H), 7.73 (d, *J* = 6.6 Hz, 1H), 7.44 (t, *J* = 9.9 Hz, 1H), 6.86 (s, 1H), 6.80 (dd, *J* = 6.7, 1.4 Hz, 1H), 4.63 (t, *J* = 6.8 Hz, 2H), 4.30 (dd, *J* = 8.8, 4.9 Hz, 1H), 3.81 (dd, *J* = 13.8, 4.9 Hz, 1H), 3.55 (dd, *J* = 13.8, 8.9 Hz, 1H), 3.42 (t, *J* = 6.8 Hz, 2H), 2.43 (s, 3H), 2.40 – 2.31 (m, 2H); ^{19}F NMR (376 MHz, CD$_3$OD) δ -63.20 (d, *J* = 12.7 Hz), -76.97, -110.65 (q, *J* = 12.7 Hz); ^{13}C NMR (101 MHz, DMSO) 171.4, 160.2, 161.0 (d, *J* = 260.0 Hz), 158.61, 153.2, 142.7, 138.63 (d, *J* = 3.6 Hz), 136.5, 134.26 (d, *J* = 10.5 Hz), 127.0, 126.5, 122.2 (q, *J* = 273.4 Hz), 118.78 (d, *J* = 21.8 Hz), 117.51 (dd, *J* = 33.4, 13.4 Hz), 114.6, 111.8, 55.7, 47.7, 40.5 (signal detected by HSQC as it overlaps with solvent peak), 39.5 (partially overlaps with solvent peak), 28.9, 21.8; HRMS (ESI, *m/z*): C$_{22}$H$_{24}$F$_4$N$_7$O$_5$S [M+H]$^+$ calc. 574.14 found 574.1475. [α]$_D^{25}$ = +5 (c = 1.3, DMSO).

Flow cytometry analysis of $\alpha_v\beta_3$ integrin expression

Cells were seeded at 0.35 x 10^6 cells/60 mm plate and grown for 72 h before the experiment. Cells were harvested from plates using cell dissociation reagent. $\alpha_v\beta_3$ cell surface expression was determined by flow cytometry as previously described,[33] using the LM609 antibody which binds selectively to $\alpha_v\beta_3$ integrin and detected with an Alexa Fluor 488 secondary antibody. Results are expressed as Median Fluorescence Intensity (MFI) of stained/ unstained cells (i.e. fluorescence in the presence/absence of $\alpha_v\beta_3$ antibody).

Radiotracer binding assays

Binding assays were performed as described in the literature.[27,33]

Automated synthesis of [^{18}F]12

The automated synthesis of [^{18}F]**12** was carried out on the TRACERlab FX-FN radiochemistry system as follows. No-carrier-added [^{18}F]fluoride was delivered to the system and passed through a QMA SEP-PAK light cartridge where the [^{18}F]fluoride was trapped and [^{18}O]water collected for recycling. Trapped [^{18}F]fluoride was eluted off the cartridge with a solution of Kryptofix 2.2.2 (K222)/0.1M K$_2$CO$_3$/ACN (1 mL) into a reaction vessel. The mixture

was azeotropically dried under a stream of helium and vacuum at 110°C for 4 min. The drying step was repeated with acetonitrile (1 mL) then compound **13** (2.0 mg) in anhydrous DMSO (1.0 mL) was added and the reaction mixture heated at 120°C for 20 min. At the end of the reaction a 1 mL mixture of ACN/water (35/65, v/v; 0.01% TFA) was added and the entire sample loaded onto a C_{18} Prodigy ODS-Prep column (10μm particle size; 250 x 10 mm) eluted with ACN/water (35/65, v/v; 0.01% TFA) at a flow rate of 3 mL/min. Eluate from the column was monitored for radioactivity and UV absorbance at 320 nm. The fraction containing [18F]**12** was collected in a round bottom flask containing water (40 mL) (Figure X) and the resultant mixture passed through a C_{18} SEP-PAK plus cartridge. The cartridge was rinsed with water (10 mL) and the product eluted with sterile ethanol (1 mL) and collected in sterile 0.9% saline (10 mL). Finally, the product was dispensed into a sterile vial *via* a 0.2 micron sterile filter for preclinical application. The radiochemical purity of the product was determined by HPLC using a C_{18} Prodigy ODS (3) column (5 μm particle size; 250 x 4.6 mm) eluted with ACN/water (35/65, v/v; 0.01% TFA) at a flow rate of 2 mL/min. The retention time for [18F]**12** was 8.6 min.

PET/CT imaging.

Four female cba nu/nu mice were implanted with 0.1mL of a 5×10^7/mL suspension of U87 cells i/d on the back. Tumors were measured daily once since a palpable tumour became apparent. Once tumors reached approx. 500mm³, PET scans were performed to assess [18F]**12** tracer uptake and biodistribution. Mice were anaesthetized by placing in an induction chamber and turning the isoflurane to 2% (oxygen at 2L/min). Mice were transferred to an anesthetic facemask on a heated bed and settled for 5 minutes and the tail vein dilated and catheterized. Mice were then transferred to the temperature-controlled imaging bed and attached to the anesthetic facemask. After CT scanning, 10-15MBq [18F]**12** in a total volume < 200μL was injected i/v. Imaging commenced immediately after tracer injection, during which time body temperature and depth of anesthesia were monitored using readouts from the imaging bed. At the end of PET scanning, the mice will be removed from the scanner and sacrificed. Tumors were excised and sectioned for autoradiography and immunohistochemistry. Inveon acquired data: before reconstruction, the list-mode data were histogrammed with a span of 3 and maximum ring differences of 79 into 3D sinograms with 19 time frames (5 × 60 seconds (s), 5 × 120s, 5×300s and 4 × 300s) for image reconstruction. Images were reconstructed using the 3D-OSEM/MAP algorithm (4 OSEM3D iterations and no MAP iterations, with a requested resolution of 1.5mm). Regions of interest (ROIs) were drawn manually over tumors using Inveon Research Workplace software (Siemens, Germany) and further normalization was performed using the injected dose (from the dose calibrator) and animal weight to give a standardized uptake value (SUV). SUVmax was calculated from the maximum voxel value within the ROI and SUVmean as the average over all voxels.

Autoradiography

Sections of flash-frozen U87 tumors cut at 20μm on a cryotome and mounted on slides were pre-incubated in Tris-NaCl at 4°C for 5 mins. The slides were then incubated for 1 hour in Tris-NaCl plus ligands at room temp (50MBq of [18F]**12** in 50mL Tris-NaCl in both, plus 2 mL of 100ug/mL cold [18F]**12** for non-specific binding test). The slices were rinsed with 2x5 mins in Tris-NaCl at 4°C, then quickly rinsed in H_2O at 4°C. Slides were prepared for phosphor-imager (FujiFilm BAS-1800 II) and exposed overnight.
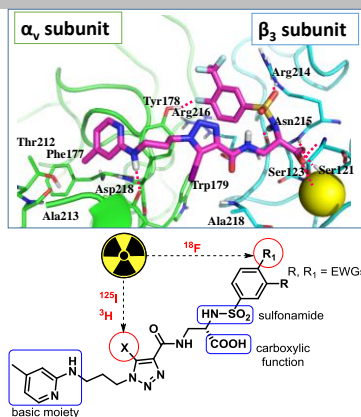
Acknowledgements

Keywords:

[1] M. Shimaoka, T. A. Springer, *Nat. Rev. Drug Discov.* **2003**, *2*, 703–716.
[2] H. Hamidi, M. Pietilä, J. Ivaska, *Br. J. Cancer* **2016**, *115*, 1017–1023.
[3] P. C. Brooks, R. A. Clark, D. A. Cheresh, *Science* **1994**, *264*, 569–571.
[4] D. Arosio, C. Casagrande, *Adv. Drug Deliv. Rev.* **2016**, *97*, 111–143.
[5] J. D. Humphries, A. Byron, M. J. Humphries, *J. Cell Sci.* **2006**, *119*, 3901–3903.
[6] J.-P. Xiong, T. Stehle, R. Zhang, A. Joachimiak, M. Frech, S. L. Goodman, M. A. Arnaout, *Science* **2002**, *296*, 151–155.
[7] L. Marinelli, A. Lavecchia, K.-E. Gottschalk, E. Novellino, H. Kessler, *J. Med. Chem.* **2003**, *46*, 4393–4404.
[8] C. Mas-Moruno, F. Rechenmacher, H. Kessler, *Anticancer Agents Med. Chem.* **2010**, *10*, 753–768.
[9] R. Haubner, D. Finsinger, H. Kessler, *Angew. Chem. Int. Ed. Engl.* **1997**, *36*, 1374–1389.
[10] W. J. Pitts, J. Wityak, J. M. Smallheer, A. E. Tobin, J. W. Jetter, J. S. Buynitsky, P. P. Harlow, K. A. Solomon, M. H. Corjay, S. A. Mousa, et al., *J. Med. Chem.* **2000**, *43*, 27–40.
[11] D. Heckmann, A. Meyer, L. Marinelli, G. Zahn, R. Stragies, H. Kessler, *Angew. Chem. Int. Ed Engl.* **2007**, *46*, 3571–3574.
[12] A. Trabocchi, G. Menchi, N. Cini, F. Bianchini, S. Raspanti, A. Bottoncetti, A. Pupi, L. Calorini, A. Guarna, *J. Med. Chem.* **2010**, *53*, 7119–7128.
[13] G. A. Sulyok, C. Gibson, S. L. Goodman, G. Hölzemann, M. Wiesner, H. Kessler, *J. Med. Chem.* **2001**, *44*, 1938–1950.
[14] W. H. Miller, R. M. Keenan, R. N. Willette, M. W. Lark, *Drug Discov. Today* **2000**, *5*, 397–408.
[15] L. Peng, R. Liu, J. Marik, X. Wang, Y. Takada, K. S. Lam, *Nat. Chem. Biol.* **2006**, *2*, 381–389.
[16] T. D. Harris, S. Kalogeropoulos, T. Nguyen, S. Liu, J. Bartis, C. Ellars, S. Edwards, D. Onthank, P. Silva, P. Yalamanchili, et al., *Cancer Biother. Radiopharm.* **2003**, *18*, 627–641.
[17] B.-S. Jang, E. Lim, S. Hee Park, I. S. Shin, S. N. Danthi, I. S. Hwang, N. Le, S. Yu, J. Xie, K. C. P. Li, et al., *Nucl. Med. Biol.* **2007**, *34*, 363–370.
[18] H. Chen, G. Niu, H. Wu, X. Chen, *Theranostics* **2016**, *6*, 78–92.
[19] N. Withofs, R. Hustinx, *Médecine Nucl.* **2016**, *40*, 41–54.
[20] J. Shi, F. Wang, S. Liu, *Biophys. Rep.* **2016**, *2*, 1–20.
[21] S. Neubauer, F. Rechenmacher, A. J. Beer, F. Curnis, K. Pohle, C. D'Alessandria, H.-J. Wester, U. Reuning, A. Corti, M. Schwaiger, et al., *Angew. Chem. Int. Ed.* **2013**, *52*, 11656–11659.
[22] F. Bianchini, P. Fabbrizzi, G. Menchi, S. Raspanti, A. Bottoncetti, A. Passeri, E. Andreucci, A. Guarna, L. Calorini, A. Pupi, et al., *Bioorg. Med. Chem.* **2015**, *23*, 1112–1122.
[23] A. Testa, M. Piras, M. Hickey, I. Fleming, N. Bushby, E. Lenz, C. Elmore, M. Zanda, *Synlett* **2014**, *25*, 1019–1025.
[24] R. Yan, E. El-Emir, V. Rajkumar, M. Robson, A. P. Jathoul, R. B. Pedley, E. Årstad, *Angew. Chem. Int. Ed.* **2011**, *50*, 6793–6795.
[25] J. Becaud, L. Mu, M. Karramkam, P. A. Schubiger, S. M. Ametamey, K. Graham, T. Stellfeld, L. Lehmann, S. Borkowski, D. Berndorff, et al., *Bioconjug. Chem.* **2009**, *20*, 2254–2261.
[26] M. E. Solomon, C. L. Lynch, D. H. Rich, *Tetrahedron Lett.* **1995**, *36*, 4955–4958.
[27] M. Piras, I. Fleming, W. Harrison, M. Zanda, *Synlett* **2012**, *23*, 2899–2902.

[28]   J. Zhu, B.-H. Luo, T. Xiao, C. Zhang, N. Nishida, T. A. Springer, *Mol. Cell* **2008**, *32*, 849–861.
[29]   P. A. Greenidge, C. Kramer, J.-C. Mozziconacci, R. M. Wolf, *J. Chem. Inf. Model.* **2013**, *53*, 201–209.
[30]   M. Mori, F. Manetti, M. Botta, *J. Chem. Inf. Model.* **2011**, *51*, 446–454.
[31]   R. Wang, L. Lai, S. Wang, *J. Comput. Aided Mol. Des.* **2002**, *16*, 11–26.
[32]   W. Cai, Y. Wu, K. Chen, Q. Cao, D. A. Tice, X. Chen, *Cancer Res.* **2006**, *66*, 9673–9681.
[33]   S. Dall'Angelo, Q. Zhang, I. N. Fleming, M. Piras, L. F. Schweiger, D. O'Hagan, M. Zanda, *Org. Biomol. Chem.* **2013**, *11*, 4551–4558.
[34]   M. R. Battle, J. L. Goggi, L. Allen, J. Barnett, M. S. Morrison, *J. Nucl. Med.* **2011**, *52*, 424–430.

Entry for the Table of Contents

FULL PAPER

Small-molecule 'click' RGD-ligands displayed excellent *in vitro* properties and offer a variety of radiolabeling options (including [^{18}F]). Binding mode to $\alpha_v\beta_3$ or $\alpha_{IIb}\beta_3$ receptors was studied by molecular modeling. Radiofluorination and PET/CT studies on **12** in tumour models showed that these mimics are excellent radiolabeled probes for *in vitro* and cell-based studies on $\alpha_v\beta_3$ integrin, but further pharmaco-kinetic and dynamic profiling is required for *in vivo* imaging.

M. Piras,* A. Testa, I. N. Fleming, S. Dall'Angelo, A. Andriu, S. Menta, M. Mori, G. D. Brown, D. Forster, K. J. Williams, and M. Zanda*

High Affinity "Click" RGD Peptidomimetics as Radiolabeled Probes for Imaging $\alpha_v\beta_3$ Integrin